J|A|C|S
ARTICLES
Published on Web 03/02/2004

Directed Self-Assembly of Monodisperse Phospholipid Bilayer Nanodiscs with Controlled Size

I. G. Denisov,[†,‡] Y. V. Grinkova,[†,‡] A. A. Lazarides,[§] and S. G. Sligar*[,†,‡,||]

Contribution from the Departments of Biochemistry and Chemistry and the Beckman Institute, University of Illinois, Urbana, Illinois 61801, and Department of Mechanical Engineering and Materials Science, Duke University, Durham, North Carolina 27708

Received October 31, 2003; E-mail: s-sligar@uiuc.edu.

Abstract: Using a recently described self-assembly process (Bayburt, T. H.; Grinkova, Y. V.; Sligar, S. G. *Nano Letters* **2002**, *2*, 853−856), we prepared soluble monodisperse discoidal lipid/protein particles with controlled size and composition, termed Nanodiscs, in which the fragment of dipalmitoylphosphatidylcholine (DPPC) bilayer is surrounded by a helical protein belt. We have customized the size of these particles by changing the length of the amphipathic helical part of this belt, termed membrane scaffold protein (MSP). Herein we describe the design of extended and truncated MSPs, the optimization of self-assembly for each of these proteins, and the structure and composition of the resulting Nanodiscs. We show that the length of the protein helix surrounding the lipid part of a Nanodisc determines the particle diameter, as measured by HPLC and small-angle X-ray scattering (SAXS). Using different scaffold proteins, we obtained Nanodiscs with the average size from 9.5 to 12.8 nm with a very narrow size distribution (±3%). Functionalization of the N-terminus of the scaffold protein does not perturb their ability to form homogeneous discoidal structures. Detailed analysis of the solution scattering confirms the presence of a lipid bilayer of 5.5 nm thickness in Nanodiscs of different sizes. The results of this study provide an important structural characterization of self-assembled phospholipid bilayers and establish a framework for the design of soluble amphiphilic nanoparticles of controlled size.

Introduction

One of the most intriguing problems, common for physical chemistry, molecular biology, and nanoscience,[1−3] is the directed self-assembly of complex structures from similar or different components, which may include small molecules, oligomers and polymers, clusters, and nanoparticles.[4−9] Such processes and the resulting self-organization of supramolecular ordered structures apparently act as a main driving force for the phase separation and symmetry breaking in the formation of anisotropy on the mesoscopic level, from phase transitions in liquid crystals[8] to highly organized biological systems.[10−11] The processes of cooperative self-assembly critically depend on component concentrations, are very sensitive to the stoichiometric ratios in the system, and often form a hierarchy of structural levels due to domain formation and molecular recognition.[12]

Recently we have shown that all these features are essential in the self-assembly of discoidal nanoparticles formed by synthetic lipids and amphipathic α-helical proteins, termed membrane scaffold proteins (MSPs).[13,14] We designed different MSPs using the human apolipoprotein A-1 (apo A-1) sequence as a template. Apolipoproteins are composed of amphipathic helices and readily form water-soluble supramolecular complexes with lipids and cholesterol derivatives.[15] Such complexes, for example the high-density and low-density lipoproteins, have an almost continuous spectrum of chemical compositions and a rich structural variability in vivo. The discoidal and spheroidal complexes designated rHDL (reconstituted high-density lipoproteins) can be reassembled from purified apolipoprotein and different lipids, with or without cholesterol.[16] Such complexes have been studied for more than 30 years and the results extensively reviewed.[15−21] Other proteins also form amphipathic

* Corresponding author.
† Department of Biochemistry, University of Illinois.
‡ Beckman Institute, University of Illinois.
§ Duke University.
|| Department of Chemistry, University of Illinois.

(1) Lehn, J.-M. *Science* **2002**, *295*, 2400−2403.
(2) Whitesides, G. M.; Mathias, J. P.; Seto, C. T. *Science* **1991**, *254*, 1312−1319.
(3) Whitesides, G. M.; Grzybowski, B. *Science* **2002**, *295*, 2418−2421.
(4) Walker, S. A.; Kennedy, M. T.; Zasadzinski, J. A. *Nature* **1997**, *387*, 61−64.
(5) Zastavker, Y. V.; Asherie, N.; Lomakin, A.; Pande, J.; Donovan, J. M.; Schnur, J. M.; Benedek, G. B. *Proc. Natl. Acad. Sci. U.S.A.* **1999**, *96*, 7883−7887.
(6) Richard, C.; Balavoine, F.; Schultz, P.; Ebbesen, T. W.; Mioskowski, C. *Science* **2003**, *300*, 775−778.
(7) Ohler, B.; Revenko, I.; Husted, C. *J. Struct. Biol.* **2001**, *133*, 1−9.
(8) Kato, T. *Science* **2002**, *295*, 2414−2418.
(9) Dubois, M.; Deme, B.; Gulik-Krzywicki, T.; Dedieu, J. C.; Vautrin, C.; Desert, S.; Perez, E.; Zemb, T. *Nature* **2001**, *411*, 672−675.
(10) Bamford, D. H.; Gilbert, R. J.; Grimes, J. M.; Stuart, D. I. *Curr. Opin. Struct. Biol.* **2001**, *11*, 107−113.
(11) Williamson, J. R. *RNA* **2003**, *9*, 165−167.
(12) Ikkala, O.; ten Brinke, G. *Science* **2002**, *295*, 2407−2409.
(13) Segrest, J. P. *Chem. Phys. Lipids* **1977**, *18*, 7−22.
(14) Bayburt, T. H.; Grinkova, Y. V.; Sligar, S. G. *Nano Letters* **2002**, *2*, 853−856.
(15) Segrest, J. P.; Garber, D. W.; Brouillette, C. G.; Harvey, S. C.; Anantharamaiah, G. M. In *Advances in Protein Chemistry*; Schumaker, V. N., Ed.; Academic Press: New York, 1994; Vol. 45, pp 303−369.
(16) Jonas, A. *Methods Enzymol.* **1986**, *128*, 553−582.

helices,[15] such as synucleins,[22] apolipophorins,[23] melittin,[24] and apomyoglobin.[25] The rapidly growing experimental evidence suggest that such proteins and synthetic oligopeptides interact with lipid bilayers and readily form intermolecular aggregates, very often in the form of supramolecular assemblies with hierarchical structural levels.[24−26]

Despite the vast amount of information and generally accepted methods for the formation of rHDL, several key features of these particles, as well as of the process of their self-assembly from the components, are still not clear. Many different sizes of discoidal protein−lipid particles for the same protein and lipid composition have been reported in the literature, with diameters from approximately 78 to 115 Å.[16,19] This is more than a 2-fold difference in the ratio of volumes of protein and lipid phase and the molecular mass of the particles. In addition, there is no general agreement about the detailed structure of the protein in such discoidal particles and about the role of the N-terminal and C-terminal parts of the apo A-1 protein which forms the HDL particles.[21] The most widely accepted model is that of two amphipathic helical belts that protein forms around a discoidal lipid bilayer structure.[21]

In this work we report new information obtained on a set of systematically varied derivatives of MSP which support such lipid bilayer self-assembly in solution. The general principles of self-assembly of a specific scaffold protein, MSP1, with phospholipids to form ∼10 nm diameter disks were recently described.[14] For many situations involving the incorporation of large membrane protein assemblies, larger discoidal bilayer structures are desired. We designed a series of extended scaffold proteins with one, two, or three additional 22-mer amphipathic helices inserted in the central part of MSP1 (designated MSP1E1, MSP1E2, and MSP1E3 correspondingly) and studied the self-assembly of discoidal particles with the cylindrical fragment of the DPPC bilayer at the center, surrounded by each of these proteins of different size, as shown schematically in Figure 1. We optimized the conditions of self-assembly to obtain the monodisperse nanoparticles, termed Nanodiscs, with each of these proteins and have shown that the length of the protein is the determinant of the particle diameter. In addition we measured the stoichiometry of lipid and protein in these particles and demonstrated that the dependence of this ratio on the length of the scaffold protein is dictated by the discoidal structure of the particles. Small-angle X-ray scattering (SAXS) data of these Nanodiscs formed with scaffold proteins of different size provide an important structural characterization of these particles. We also prepared the series of deletion mutant scaffold proteins, in which up to 22 N-terminal amino acids were deleted from the MSP1 sequence. The same set of experiments with Nanodiscs

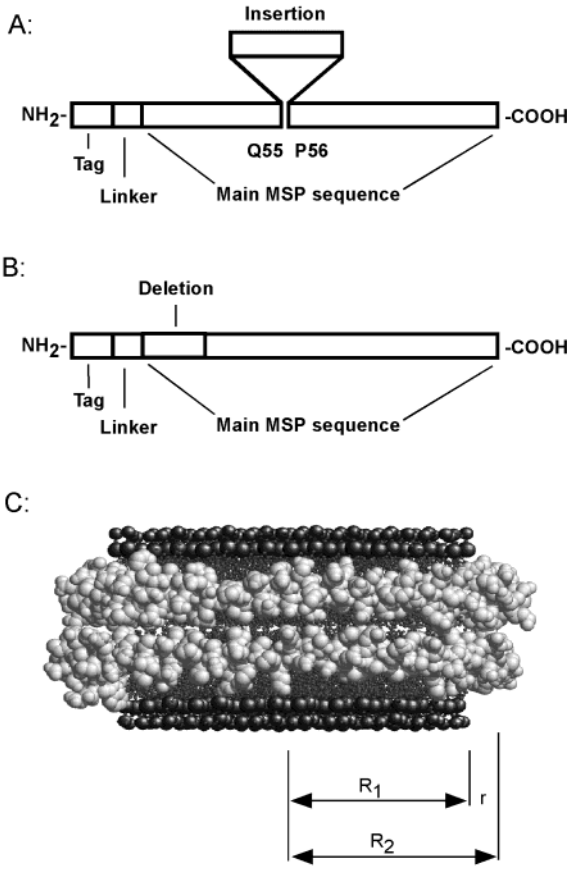

Figure 1. (A) Schematic representation of the initial MSP1 (**1**) and extended membrane scaffold proteins, MSP1E1, MSP1E2, and MSP1E3 (**2**−**4**). (B) Schematic representation of truncated membrane scaffold proteins MSP1 (**5**−**11**). (C) Model of Nanodisc, the discoidal lipid/protein particle with a cylindrical fragment of lipid bilayer in the center and two helical protein molecules around the lipid part: R_1, radius of the lipid cylinder; r, average radius of protein α-helix; R_2, radius of the circle formed by the axis of the protein helix.

formed with the truncated proteins suggest that these deleted amino acids are not necessary for the self-assembly of these discoidal lipid bilayer structures and do not take part in forming the encircling "belt" that stabilizes the bilayers in solution. This result was unanticipated given the extensive literature on related experiments with human apolipoproteins in high-density lipoprotein structures and points toward a rational engineering of membrane scaffold proteins for novel uses of solubilized phospholipids nanostructures.

Experimental Section

Chemicals. The lipids 1,2-dipalmitoyl-*sn*-glycero-3-phosphocholine (DPPC) and 1-palmitoyl-2-oleoyl-*sn*-glycero-3-phosphocholine (POPC) were purchased from Avanti Polar Lipids (Alabaster, AL), ^{3}H-DPPC was from American Radiolabeled Chemicals (St. Louis, MO). All other chemicals were from Sigma-Aldrich or Fisher. Restriction enzymes and DNA-modifying enzymes were purchased from New England Biolabs (Beverly, MA) or Invitrogen (Carlsbad, CA). Water was purified with a Milli-Q purification system (Millipore, Billerica, MA).

Extended Scaffold Proteins. The sequences of new scaffold proteins were designed on the basis of the model shown in Figure 1 and selected by taking into account the salt link score for the belt model of the antiparallel dimer as described.[27] At first, the amino acid sequences of the extended mutants were generated so that each of the central 22-mer helical repeats punctuated by prolines P56, P78, P100, and P122, corresponding to the MSP1 sequence (see Supporting Information for

(17) Laggner, P.; Muller, K. W. *Q. Rev. Biophys.* **1978**, *11*, 371−425.
(18) Brouillette, C. G.; Anantharamaiah, G. M.; Engler, J. A.; Borhani, D. W. *Biochim. Biophys. Acta* **2001**, *1531*, 4−46.
(19) Brouillette, C. G.; Anantharamaiah, G. M. *Biochim. Biophys. Acta* **1995**, *1256*, 103−129.
(20) Atkinson, D.; Small, D. M. *Annu. Rev. Biophys. Biophys. Chem.* **1986**, *15*, 403−456.
(21) Klon, A. E.; Segrest, J. P.; Harvey, S. C. *Biochemistry* **2002**, *41*, 10895−10905.
(22) Zhu, M.; Fink, A. L. *J. Biol. Chem.* **2003**, *278*, 16873−16877.
(23) Garda, H. A.; Arrese, E. L.; Soulages, J. L. *J. Biol. Chem.* **2002**, *277*, 19773−19782.
(24) Posch, M.; Rakusch, U.; Mollay, C.; Laggner, P. *J. Biol. Chem.* **1983**, *258*, 1761−1766.
(25) Lee, J. W.; Kim, H. *Arch. Biochem. Biophys.* **1992**, *297*, 354−361.
(26) Ladokhin, A. S.; Selsted, M. E.; White, S. H. *Biophys. J.* **1997**, *72*, 1762−1766.

Table 1. Labels and Amino Acid Sequences of Membrane Scaffold Proteins Used for Self-Aassembly of Nanodiscs

scaffold protein variant	abbreviated name[a]	N-terminal tag for affinity chromatography	linker and protease recognition site[b]	insertion[c] or deletion[d]
1	MSP1	MGHHHHHH	IEGA	-
2	MSP1E1	same	same	MSP(56−77)[c]
3	MSP1E2	same	same	MSP(56−99)[c]
4	MSP1E3	same	same	MSP(56−121)[c]
5	MSP1TEV	MGHHHHHH	DYDIPTTENLYFQG	-
6	MSP1(−)	-	G	
7	MSP1D1	MGHHHHHH	DYDIPTTENLYFQG	MSP(1−11)[d]
8	MSP1D1(−)	-	G	MSP(1−11)[d]
9	MSP1D2	MGHHHHHH	DYDIPTTENLYFQG	MSP(1−22)[d]
10	MSP1D2-P23S	same	same	MSP(1−22)[d], *P23S*[e]
11	MSP1D2-P23S(−)	-	G	MSP(1−22),[d] *P23S*[e]

[a] Abbreviated names: (**1**) MSP1, membrane scaffold protein 1 [14] with N-terminal hexa-His tag, followed by Factor X recognition site. The sequence of MSP1 contains 200 amino acids and is listed in Supporting Information. (**2**−**4**) MSP1E1, MSP1E2, MSP1E3, extended membrane scaffold proteins, obtained via insertion of one (residues 56−77 of original MSP1), two (residues 56−99), or three (residues 56−121) extra 22-mer amphipathic helices after the residue Q55 into the original MSP1 (**1**) sequence, as described in the Experimental Section. All have N-terminal hexa-His tag and Factor X recognition site. (**5**) MSP1TEV, MSP1 with N-terminal hepta-His tag, TEV protease recognition site and linker. (**6**) MSP1(−), MSP1 with no N-terminal tag. (**7**) MSP1D1, MSP1 with the first 11 N-terminal amino acids removed which contains the N-terminal hepta-His tag and TEV protease recognition site with linker. (**8**) MSP1D1(−), same as structure **7**, with no tag. (**9**) MSP1D2, MSP1 with the first 22 N-terminal amino acids removed contains the N-terminal hepta-His tag and TEV protease recognition site with linker. (**10**) MSP1D2-P23S, same as structure **9**, with Pro23 replaced by Ser. (**11**) MSP1D2(−)P23S, same as structure **10**, but no N-terminal tag. [b] Protease recognition site for removal of N-terminal hexa-His, or hepta-His tags, engineered for affinity chromatography purification of corresponding scaffold proteins or lipid−protein particles formed with these scaffold proteins, **1**−**4**. IEGA, recognition site for Factor X. **5, 7**, **9**, and **10**. DYDIPTT is the linker between the hepta-His tag and the following TEV protease recognition site ENLYFQG.[28] **6**, **8**, and **11**—no tag, serves as a control to show that the presence of tag and linker does not change the size and composition of lipid−protein particles; see Results. [c] Sequences of the main structural features of the membrane scaffold proteins are represented using enumeration corresponding to the initial MSP1 sequence **1** as described.[14] Extended scaffold proteins **2**−**4** are generated by insertion of the indicated fragment of MSP1 between residues Q55 and P56. [d] Truncated scaffold proteins are obtained by deletion of the indicated N-terminal fragment of MSP1. Hepta-His tag with TEV protease recognition site and linker were engineered in scaffold proteins **7**, **9**, and **10**, as shown. [e] Mutation of proline-23 to serine was used to facilitate cleavage of the tag, catalyzed by TEV protease, as described in the Experimental Section.

details), was inserted sequentially at every position between other central helices. The number of favorable salt links minus the number of unfavorable contacts of the same charges was calculated for all possible configurations of antiparallel dimers in the resulting scaffold protein, modeled as an ideal helical belt around the cylindrical fragment of lipid bilayer, schematically illustrated in Figure 1. From this approach, an insertion site between glutamine-55 and proline-56 was selected to generate the extended mutants **2**−**4**, Table 1.

Cloning and Mutagenesis. Plasmids for expression of extended MSPs were constructed from plasmid for MSP1 as described previously,[14] using a Seamless cloning kit (Stratagene, La Jolla, CA) according to manufacturer recommendations. The MSP1 protein sequence was designed with a 6-His affinity tag and Factor Xa recognition site (Table 1, proteins **1**−**4**). However, removal of the affinity tag with Factor Xa protease turned out to be difficult because nonspecific cleavage occurred outside of the recognition site. To improve yield, we have changed the N-terminal sequence of MSP1 to incorporate the tobacco etch virus (TEV) protease recognition site (Table 1, proteins **5**, **7**, **9**, and **10**). An alternative N-terminus was added by PCR; the primers were designed to include Nco I and Hind III restriction sites. The PCR product was digested with these restriction enzymes and cloned into pET-28a plasmid (Novagen, Madison, WI). Truncation mutants of MSP were produced with a Quick-change kit (Stratagene) using the MSP1TEV plasmid as a template. Presence of the desired insertions or deletions and absence of PCR-induced mutations were verified by DNA sequencing.

Protein Expression and Purification. MSP expression and purification was carried out as described previously.[14] Protein purity was characterized by SDS−PAGE and electrospray mass spectrometry and was found to be greater than 95%. The TEV protease expression system was purchased from Science Reagents, Inc. (El Cajon, CA). Expression and purification was generally performed as described elsewhere.[28] MSP without the His tag (**6**, **8**, and **11**) were prepared from proteins **5**, **7**, and **9** by treatment with TEV protease followed by purification on a Ni-chelating column. To achieve efficient cleavage in MSP2D2, proline-23 was mutated to serine.

Preparation of the Disk Samples. The general procedure for self-assembly of Nanodiscs is the same as that described previously.[14] Briefly, the solution of purified MSP at 0.15−0.3 mM concentration was combined with cholate-solubilized DPPC to yield an optimal molar ratio, previously estimated from small-scale experiments. After incubation at 38 °C, the self-assembly process is initiated by dialysis against 1000-fold excess of buffer at the same temperature using 10 000 MW cutoff membranes.

Analytical Procedures. Concentrations of lipids were measured using tritiated lipids of the same chemical structure and scintillation counting of the column fractions, as described.[14] The specific activity of each batch of radioactive lipids was determined by quantitation of phosphate[29] and scintillation counting using standard procedures. For calibration we used standard phosphorus solutions (Sigma, P3869) and [1,2-^{3}H]hexadecanol (Moravek Biochemicals, Brea, CA). Concentrations of scaffold proteins were determined using molar absorption coefficients calculated for the known amino acid sequences according to published methods.[30] Assembled Nanodiscs were size-separated by HPLC (Millenium System, Waters, Milford, MA) on a calibrated size exclusion chromatography (SEC) column with Superdex 200 HR 10/30 (Amersham Biosciences, Piscataway, NJ). Data were processed and analyzed using the GRAMS/AI software package (ThermoGalactic, Salem, NH). Chromatographic bands corresponding to the main Nanodisc fraction appeared symmetrical, and their positions are reported as the positions of corresponding maxima following the absorbance at 280 nm.

SAXS Measurements and Analysis. Small-angle X-ray scattering was measured at the Advanced Photon Source (Argonne National Laboratory, Argonne, IL) at ambient temperature 293 K in a vacuum chamber, at 1.5 m distance from the sample to the 2D detector, and a nominal photon energy of 15 keV (wavelength 0.826 Å). The solutions of the Nanodiscs were sealed in glass capillaries with diameter 1.5 mm (Charles Supper Co., Natick, MA) and placed in the sample chamber.

(27) Segrest, J. P.; Jones, M. K.; Klon, A. E.; Sheldahl, C. J.; Hellinger, M.; De Loof, H.; Harvey, S. C. *J. Biol. Chem.* **1999**, *274*, 31755−31758.
(28) Kapust, R. B.; Tozser, J.; Copeland, T. D.; Waugh, D. S. *Biochem. Biophys. Res. Commun.* **2002**, *294*, 949−955.
(29) Chen, P. S.; Toribara, T. Y.; Warner, H. *Anal. Chem.* **1956**, *28*, 1756−1759.
(30) Pace, C. N.; Vajdos, F.; Fee, L.; Grimsley, G.; Gray, T. *Protein Sci.* **1995**, *4*, 2411−2423.

Silver behenate with spacing 58.38 Å [31] was used for calibration, and reference buffer solvents were for background correction. The raw data were processed using the program FIT2D[32,33] to give the scattering curves in the form $\log(I/I_0)$ vs $Q = 4\pi \sin(\theta)/\lambda$. Analysis of SAXS data used the programs GNOM[34] and CRYSOL[35] and subroutines written in MATLAB (MathWorks, Natick, MA). The fitting programs used analytical expressions derived for symmetrical core−shell models (spheres, cylinders, and ellipsoids)[36] or Debye equation and modeling of the nanoparticle by close packed spherical beads with different contrast, similar to the popular programs CRYSOL, DUMMIN, SAXS3D, and DALAI·GA, which have been reviewed.[37,38] The models for fitting were constructed using the information on size and composition of Nanodiscs obtained by other methods described in this paper. Four layers with different electron density were used in these models, one for the protein and three for the lipid bilayer, namely, phosphocholine polar heads, acyl chains, and methylene end groups at the center of the bilayer.[39] The initial guess for the scattering contrasts, i.e., the differences between the electron density for water, 0.334 e/Å^{-3} and the average electron densities for the methylene groups in the central part of bilayer (−0.12 e/Å^{-3}), lipid acyl chains (−0.04 e/Å^{-3}), lipid polar headgroups (0.12 e/Å^{-3}),[39] and scaffold protein at the circumference of the particle (0.11 e/Å^{-3}),[40] were assigned to each bead representing correspondent phases. Experimental curves for each type of Nanodiscs were fitted with no additional constraints using six parameters, four electron densities, the bilayer thickness, and the radius of the disk. No attempt to introduce size or shape heterogeneity into the fitting was made. Modeling of such heterogeneity within 5% diameter changes, the maximum possible heterogeneity limits suggested by other experimental data in this study did not give a large difference in calculated scattering curves, although more significant variance in size and shape resulted in the loss of observed features on the scattering curves and gave considerably poorer fits.

Results

Using the membrane scaffold protein MSP1, which has been described in detail,[14] we designed, expressed, and purified a series of engineered amphipathic helical proteins with systematically varied amino acid sequences. These are compiled in Figure 1 and Table 1. The goal of this effort was to explore the possibility of controlling the size of self-assembled lipid−protein particles through variation of the length of the scaffold protein and to study the influence of the N-terminal residues, including the additional histidine tags, on the formation of Nanodiscs. Three new extended scaffold proteins were created using insertions of additional amphipathic helical 22-mer segments which were copied from the central part of initial MSP1 sequence. Several different N-terminal deletion mutants with or without a removable histidine tag and a TEV protease recognition site at the N-terminus were also created. Synthetic genes coding for these proteins were cloned and expressed as described in Experimental Section. All proteins were used in self-assembly of lipid−protein nanoparticles in aqueous solution, which were thoroughly studied with respect to the size, composition, and structure of the Nanodiscs resulting from the self-assembly procedure.

The self-assembly of the protein−lipid particles initiated by gradual removal of cholate using dialysis can produce a mixture of aggregates of different sizes and composition with the overall yield dependent on both the absolute concentrations of components and their ratios. However, for optimized lipid to scaffold protein ratios, a homogeneous particle size is produced.[14] Our self-assembly products were analyzed on a size exclusion HPLC column, using optical absorption spectra for detection. The conditions for the formation of homogeneous Nanodiscs were optimized for each scaffold protein listed in Table 1 in a series of small-scale preparations with different lipid/protein ratios. A typical series of such experiments is shown in Figure 2. At low lipid/protein ratios, some free protein is still detected, together with heterogeneous lipid/protein particles. With the increase of lipid fraction the system becomes more homogeneous and reaches a maximum in yield at the optimum ratio of approximately 100 lipids/protein for MSP1TEV and 150 lipids/protein for MSP1E2. Further increase of lipid content in the self-assembly mixture results in appearance of larger lipid/protein particles with a broad size distribution, although the main fraction typical for the optimal concentration ratio is usually still present.

For structural studies, Nanodiscs, monodisperse and homogeneous in compositions, were assembled from DPPC and different scaffold proteins using the optimal stoichiometric ratios of lipid and protein, which were experimentally determined for each case. Fractions from SEC separation (Experimental Section) were collected separately, and aliquots taken from the main peaks were subjected to a second fractionation to ensure complete size homogeneity. The results of this experiment are shown in Figure 3, together with the set of size calibration proteins for comparison. The chromatographic profiles of Nanodisc fractions have the same width and shape as the standard pure proteins, providing further evidence for the homogeneity of the discoidal lipid−protein particles formed with the scaffold proteins **1**−**4**, Table 1, when assembled at the optimal lipid/protein stoichiometric ratio. For all scaffold proteins the narrow range of optimal lipid/protein concentration ratio in the assembly mixture was identified with respect to the yield and size homogeneity of Nanodiscs in the main fraction. Lower (less than 75−80% of optimal) or higher (higher than 130% of optimal) lipid/protein molar ratios resulted in a lower yield in the main peak and formation of multiple species. The optimal lipid/protein ratio increased with the increase of the length of the main scaffold protein, from **1** to **4**, and was not dependent on the presence or absence of an amino terminal affinity tag.

At the optimal lipid/protein ratio the overall recovery was usually 80−95% of the total starting materials. The Stokes diameters of the particles were estimated on a Superdex 200 SEC column calibrated with a standard set of proteins, Figure 3. The linearity of calibration is based on simple model assumptions,[41,42] and experimentally observed deviations from linearity may introduce systematic errors into the sizes determined by this method.[41] Specifically, catalase with the

(31) Huang, T. C.; Toraya, H.; Blanton, T. N.; Wu, Y. *J. Appl. Crystallogr.* **1993**, *26*, 180−184.
(32) Hammersley, A. P. http://www.esrf.fr/computing/scientific/FIT2D, 1998.
(33) Hammersley, A. P.; Svensson, S. O.; Hanfland, M.; Fitch, A. N.; Häusermann, D. *High Pressure Res.* **1996**, *14*, 235−248.
(34) Svergun, D. I. *J. Appl. Crystallogr.* **1992**, *25*, 493−503.
(35) Svergun, D.; Barberato, C.; Koch, M. H. J. *J. Appl. Crystallogr.* **1995**, *28*, 768−773.
(36) Pedersen, J. S. *Adv. Colloid Interface Sci.* **1997**, *70*, 171−210.
(37) Takahashi, Y.; Nishikawa, Y.; Fujisawa, T. *J. Appl. Crystallogr.* **2003**, *36*, 549−552.
(38) Koch, M. H. J.; Vachette, P.; Svergun, D. I. *Q. Rev. Biophys.* **2003**, *36*, 147−227.
(39) Wiener, M. C.; Suter, R. M.; Nagle, J. F. *Biophys. J.* **1989**, *55*, 315−325.
(40) Svergun, D. I.; Richard, S.; Koch, M. H. J.; Sayers, Z.; Kuprin, S.; Zaccai, G. *Proc. Natl. Acad. Sci. U.S.A.* **1998**, *95*, 2267−2272.

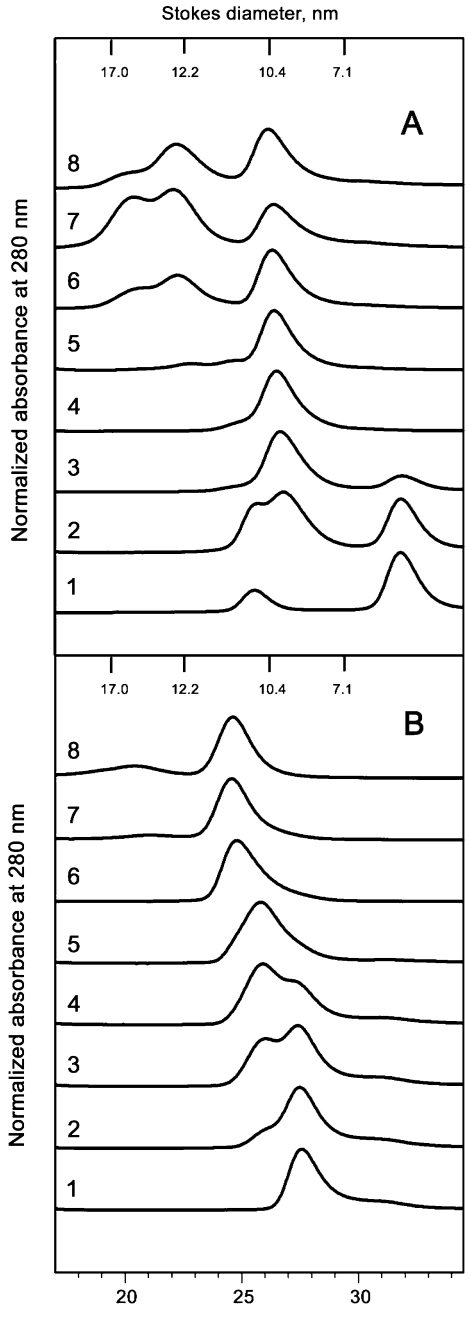

Figure 2. SEC of self-assembled Nanodiscs. HPLC separation on a Superdex 200 (Experimental Section) for different lipid/protein ratios in the self-assembly mixture is shown. The scaffold proteins used are as follows: (A) MSP1TEV (**5**); (B) MSP1E2 (**3**). The molar lipid/protein ratios for both panels are as follows: (1) 0; (2) 25; (3) 50; (4) 75; (5) 100; (6) 150; (7) 200; (8) 300.

Stokes diameter of 104 Å is detected at 99−100 Å in SEC. Based on such calibration, the Stokes diameter of Nanodiscs formed with the membrane scaffold protein **1** is determined to be 95−96 Å, although the position of the elution peak close to that of catalase suggests a slightly larger estimated diameter of about 100 Å.

We determined the average numbers of lipids per Nanodisc by scintillation counting self-assembly mixtures containing

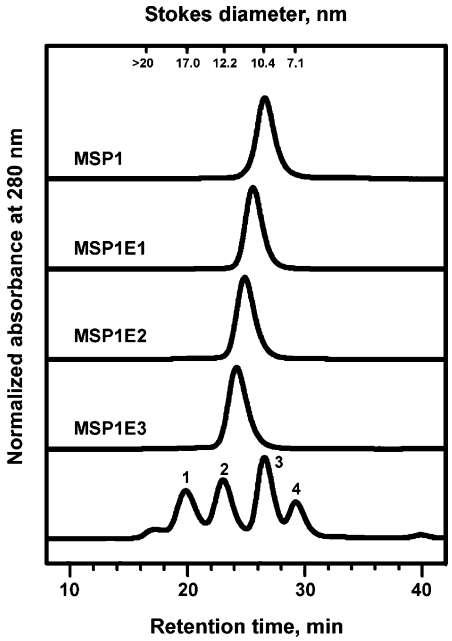

Figure 3. Elution profiles from SEC of Nanodiscs assembled with DPPC and MSP1, MSP1E1, MSP1E2, and MSP1E3. The lower chromatogram illustrates the elution profile for the set of calibration proteins with respective Stokes diametersas follows: (1) thyroglobulin, 17 nm; (2) ferritin, 12.2 nm; (3) bovine liver catalase, 10.4 nm; (4) bovine serum albumin, 7.1 nm. The resulting calibrated Stokes diameter scale is shown at the top of the figure.

Table 2. Structure and Composition of Nanodiscs Formed with the Scaffold Proteins of Different Sizes

scaffold protein	DPPC/protein,[a] mol/mol	Stokes diameter,[b] nm	SAXS R_g,[c] nm	SAXS diameter,[d] nm	SAXS thickness,[d] nm
1	82 ± 1	9.7	4.6	9.8	5.6
2	106 ± 1.5	10.4	5.0	10.6	5.6
3	134 ± 3.3	11.1	5.4	11.9	5.5
4	167 ± 6	12.0	5.9	12.9	5.5
5	83 ± 1	9.7	4.6	10.0	5.9
6	80 ± 2.7	9.7	4.6	10.0	5.7
7	81 ± 1.2	9.5	4.5	9.7	5.7
8	81 ± 1.3	9.6	4.5	9.6	5.7
9	79 ± 0.8	9.6	4.5	9.7	5.9
10	78 ± 0.4	9.4	ND	ND	ND
11	75 ± 0.2	9.4	ND	ND	ND

scaffold protein	POPC/protein, mol/mol	Stokes diameter,[b] nm	SAXS R_g,[c] nm	SAXS diameter,[d] nm	SAXS thickness,[d] nm
1	61 ± 5	9.7	4.5	9.7	4.6
2	79 ± 7	10.5	ND	ND	ND
3	103 ± 7	11.3	ND	ND	ND
4	124 ± 12	12.1	6.2	12.8	4.6

[a] Calculated from independent measurements with the same samples—lipid concentrations by scintillation counting, protein—by near-UV absorption spectroscopy. [b] Data for Nanodiscs formed with DPPC calculated from HPLC data using the set of proteins shown in Figure 3 for calibration. [c] Results for Nanodiscs formed with DPPC. The radii of gyration R_g were calculated in the course of fitting of experimental curves using GNOM;[34] results are shown in Figure 4. ND = not determined [d] Diameter and thickness calculated by unconstrained fit of experimental results to the model of the Nanodisc consisting of flat cylindrical layers. The outer diameter of the Nanodisc and the thickness of the bilayer were used as fitting parameters together with four parameters describing the scattering contrast, i.e., the differences between the electron density of water, 334 e/nm^3, and those of the protein, the lipid phosphocholine polar heads, lipid acyl chains, and lipid methylene groups at the center of bilayer, as is used in fitting SAXS results for lamellar lipid phases.[39,46]

tritiated lipids, Table 2. With the scaffold proteins MSP1 and MSP1E1, the Nanodiscs were virtually homogeneous in com-

(41) Vander Heyden, Y.; Popovici, S. T.; Schoenmakers, P. J. *J. Chromatogr. A* **2002**, *957*, 127−137.
(42) Winzor, D. J. *J. Biochem. Biophys. Methods* **2003**, *26*, 15−52.

position, and the lipid/protein ratio is constant within 2−3% across the elution peak for each sample of Nanodiscs (data not shown). With MSP1E2, and especially MSP1E3, a gradual decrease of lipid/protein ratio is observed from the leading to the trailing edge of the elution peak. However, even these differences in the number of lipids per particle were always less than 20% from the leading to the trailing edge of the band. The corresponding variations in particle diameter are less than 10%, and in most cases much better, being similar to results using standard 100 nm polystyrene spheres.[43]

The expected volumes of the assembled nanobilayer structures can be calculated from the experimentally determined compositions, Table 2, and the known molecular volumes of the constituents. For example for DPPC $V = 1.15$ nm^3,[39] and for MSP1 scaffold protein **1** $V = 28.4$ nm^3, as calculated with CRYSOL based on the X-ray structure of apo A-1 (Δ1-43) truncated mutant.[44] These volumes were compared with the Stokes radii of corresponding particles, and the first estimate of possible shape can be evaluated from this comparison. For MSP1 (**1**, Table 2), the calculated volumes are 123, 246, and 368 nm^3, for lipid/protein ratio 82:1 and one, two, or three protein molecules per particle, respectively. The calculated volume of the discoidal particle with the structure illustrated in Figure 1, with a diameter of 9.8 nm and a bilayer thickness of 5 nm, is 280 nm^3, consistent with two protein molecules per particle. The following analysis and that in the Discussion strongly support a discoidal shape of the particles with two scaffold protein molecules per Nanodisc.

The data on the composition of Nanodiscs formed with extended proteins **1**−**4** (Table 2) can be used to test the structural model of the discoidal particle presented at Figure 1. Assuming a similar overall structure for particles formed with the different length scaffold proteins, a simple calculation provides a connection between the length of the protein belt around the lipid part of the Nanodisc and the number of lipids per monolayer:

$$ML = 2\pi R_2; \quad NS = \pi R_1^{\,2}; \quad R_2 - R_1 = r \qquad (1)$$

where r is the average radius of the scaffold protein amphipathic helix, N the number of lipids in one leaflet of the bilayer, S the average surface area per one lipid, M the number of residues in the helical protein belt, and L the helical pitch per residue, taken to be 1.5 Å.[45]

From eqs 1 it follows that

$$M = 2(\pi r + \sqrt{\pi NS})/L \qquad (2)$$

Assuming an average radius of the protein helix of $r = 5.5$ Å, and using the number of lipids per one protein N, which is determined experimentally (Table 2), the total length of the protein helical belt around the bilayer fragment in the disk can be calculated using eq 2 for each of the entries **1**−**4** in Table 2. The value of S is not known a priori and can be found from an additional constraint due to amino acid sequences of these proteins. For example, the resulting M values for particles of different sizes are connected by the following relation

$$M(j+1) = M(1) + 22j$$

where $j = 1$, 2, and 3—the number of helical 22-mers inserted into the MSP1 sequence to form the set of extended proteins **2**−**4**. These calculations show that for $S = 52$ Å^2, the difference between calculated values of M is $\delta M = 22$, as it has to be according to the known sequences of **1**−**4** and the structural model shown in Figure 1. This calculation also returns the length of the protein belt around the lipid in the disk formed with MSP1, M(**1**) = 177 amino acids. The precision of this value for the calculated average surface area, S, per one lipid molecule in Nanodiscs can be estimated from the following comparison of the actual difference in length between our extended proteins, $\delta M = 22$ amino acids, and the one calculated with different values for S. If $S = 48$ Å^2, which is typical for the gel state of DPPC,[46] then $\delta M = 21$ and M(**1**) = 171; if $S = 57$ Å^2, $\delta M = 23$ and M(**1**) = 184. These S values may be taken as the error limits for such estimates, thus providing an estimated length of helical protein belt around the bilayer in disks M(**1**) between 171 and 184 amino acids. This is significantly smaller than the total length of MSP1, 200 amino acids. From $S = 52$ Å^2 one may conclude that the fragment of DPPC bilayer in Nanodiscs is in the gel state, as could be expected at 295 K, well below the temperature of the main phase transition, 314 K for DPPC. The higher value of the average surface area per lipid in Nanodiscs, as compared to 48 Å^2 in bilayers, may be attributed to the structural perturbation of the lipid packing at the protein−lipid interface at the disk rim. The existence of such interfacial lipids with more disordered packing was detected earlier in similar lipid/protein particles by NMR[47] and fluorescence spectroscopy.[48]

The results of this analysis provide strong evidence for a structure with an eight-segment helical protein belt, 22 residues per helix, or a total of 176 residues, around the lipid part in Nanodiscs formed with MSP1. However, MSP1 contains 200 amino acids, not counting the N-terminal tags and spacers, as described in Experimental Section. This finding raises the question as to the role of the remainder of the protein. To answer this question, several truncated mutant MSP1 were created. The results of similar measurements with these proteins are also shown in Table 2. Comparison of all results on the lipid/protein ratio in Nanodiscs as a function of the length of the scaffold protein reveals an interesting tendency. Insertions of extra helices in the central part of the protein (MSP1E1, MSP1E2, and MSP1E3) provide the formation of disks of larger sizes, and the deletions of tags at the N-terminus and, further, of the first 22 amino acids from the first supposed helical segment do not dramatically change the number of lipids in the disks. The data in Table 2, i.e., the Stokes radii, lipid/protein stoichiometry, and solution X-ray scattering, imply very similar sizes for Nanodiscs formed (a) with original MSP1 with 6-His tag (Table 2, **1**); (b) with the same tag and longer linker to the structural protein (**5**); (c) with no tag at all (**6**); and (d) with truncated MSP1, where 11 (**7**, **8**) or 22 (**9**) amino acids are deleted. The fact that the tags, engineered at the N-termini for affinity chromatography of the disks, are not involved in the lipid/protein

(43) Mulholland, G. W.; Bauer, B. J. *J. Nanopart. Res.* **2000**, *2*, 5−15.
(44) Borhani, D. W.; Rogers, D. P.; Engler, J. A.; Brouillette, C. G. *Proc. Natl. Acad. Sci. U.S.A.* **1997**, *94*, 12291−12296.
(45) Benedetti, E.; Di Blasio, B.; Pavone, V.; Pedone, C.; Toniolo, C.; Crisma, M. *Biopolymers* **1992**, *32*, 453−456.
(46) Nagle, J. F.; Tristram-Nagle, S. *Biochim. Biophys. Acta* **2000**, *1469*, 159−195.
(47) Brouillette, C. G.; Jones, J. L.; Ng, T. C.; Kercret, H.; Chung, B. H.; Segrest, J. P. *Biochemistry* **1984**, *23*, 359−367.
(48) Dergunov, A. D.; Dobretsov, G. E. *Chem. Phys. Lipids* **2000**, *104*, 161−173.

interactions and do not form the helical belt around the lipid part of the Nanodisc could be expected, due to the absence of a predicted amphipathic helical motif in these fragments. On the contrary, the so-called first helix (residues 1−22 in MSP1, **1**) of the human apolipoprotein apo A-1 was usually presumed to be an essential part of the scaffold protein in modeling of analogous discoidal particles.[21] This assumption apparently was based on the fact that all except five residues from N-terminus form α-helix in the crystal structure of the similar protein, truncated apo A-1.[44] However, no systematic experimental study such as that reported herein has been previously conducted with regard to the structure and composition of such disks formed with extended and truncated proteins.

The data shown in Table 2 strongly suggest that the first 20−22 amino acids are marginally, if at all, involved in the formation of the Nanodisc. As evidenced by the assembly stoichiometry and HPLC hydrodynamic measurements, Nanodiscs of different sizes all have similar structure, which is consistent with the scaffold protein forming a continuous helical belt around the lipid bilayer beginning from residues 20−22 in the MSP1. This geometry results in a quadratic increase of the number of lipids per disk with respect to the number of amino acids in the protein belt at the disk rim. Analysis of our experimental data for the series of extended scaffold proteins **1**−**4** using eq 2 shows very good agreement with this model.

The results just described used DPPC as phospholipids which form as gel-phase structures at room temperature. However, the same results were obtained using POPC, which has a lower transition temperature, 270 K, and is at liquid crystalline state at ambient conditions. POPC data are also shown in Table 2. The sizes of Nanodiscs formed with POPC are identical to corresponding disks with DPPC, confirming that the length of the scaffold protein solely determines the diameter of discoidal particle. The difference in the number of POPC and DPPC molecules per Nanodisc is explained by the equilibrium properties of corresponding bilayers. Specifically, the mean surface area per lipid molecule for DPPC is estimated from Table 2 and eq 2 to be 52 Å^2 and for POPC 69 Å^2, consistent with our earlier data[14] and in very good agreement with the X-ray studies of lamellar phases. Taken together, these data show that the size and composition of self-assembled Nanodiscs can be tuned by the proper choice of length of the scaffold protein and the lipid with known physical properties. Moreover, the optimal ratio of protein and lipid concentrations in the initial self-assembly mixture can be predicted for other systems on the basis of the known length of the protein and the mean surface area per lipid in the given conditions. We have recently confirmed the general validity of these rules using different lipids and various scaffold proteins. Thus, the results in Table 2, together with successful fits to eq 2, reveal the factors which determine the size of Nanodiscs and the optimal stoichiometry for the given pair of the scaffold protein and lipid, as well as the composition of resulting discoidal particles resulting from self-assembly.

To obtain more detailed and direct structural information on the size and composition of Nanodiscs, SAXS was measured for the samples **1**−**9**. These results are shown in Table 1 and Table 2. The scattering curves obtained for disks of different sizes, formed with extended scaffold proteins, are shown in Figure 4A. The shape of these curves with sharp minimum and broad maximum is typical for discoidal particles, or for oblate

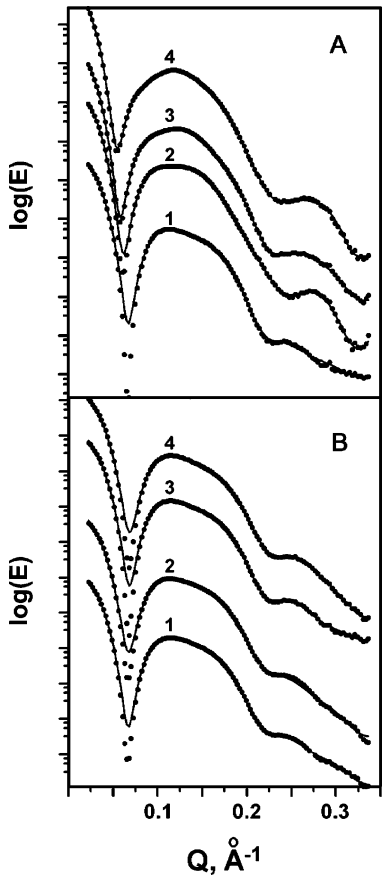

Figure 4. Small-angle X-ray scattering from Nanodiscs formed with DPPC and the following proteins. Panel A: 1, MSP1 (**1**); 2, MSP1E1 (**2**); 3, MSP1E2 (**3**); 4, MSP1E3 (**4**). Panel B: 1, MSP1NH (**6**); 2, MSP1TEV (**5**); 3, MSP1D1 (**7**); 4, MSP1D2 (**9**). Data points are shown explicitly with the solid curves being the results of theoretical fitting (see text).

ellipsoids, as was reported in earlier studies of lipoproteins.[17,49] Indeed, similar SAXS results were reported for discoidal phospholipid micelles stabilized by different surfactants in aqueous solution, often called bicelles.[34,50−53]

The results of fitting procedures using GNOM[34] (see Experimental Section) are also shown in Figure 4A. This program calculates the distance distribution function of the scattering particle, containing information on the distribution of scattering contrast over the volume of the particle or the difference between the electron density of the particle and that of solvent water (334 e/nm^3). This difference is negative for the central part of the lipid bilayer, since saturated hydrocarbons have lower electron density, and positive for protein and phosphocholine polar heads, which both have higher electron density than water.[54] This structural feature of lipid bilayers results in characteristic minima of the distance distribution functions as shown in Figure 5, and significantly higher values of the radius of gyration, R_g, than those for homogeneous particles with the

(49) Atkinson, D.; Smith, H. M.; Dickson, J.; Austin, J. P. *Eur. J. Biochem.* **1976**, *64*, 541−547.
(50) Funari, S. S.; Nuscher, B.; Rapp, G.; Beyer, K. *Proc. Natl. Acad. Sci. U.S.A.* **2001**, *98*, 8938−8943.
(51) Taya, K.; Kuboa, K.; Ochiai, K.; Wakamatsu, K. *Trans. Mater. Res. Soc. Jpn.* **2002**, *27*, 605−608.
(52) Bolze, J.; Fujisawa, T.; Nagao, T.; Norisada, K.; Saito, H.; Naito, A. *Chem. Phys. Lett.* **2000**, *329*, 215−220.
(53) Somjen, G. J.; Coleman, R.; Koch, M. H. J.; Wachtel, E.; Billington, D.; Towns-Adrews, E.; Gilat, T. *FEBS Lett.* **1991**, *289*, 163−166.
(54) Feigin, L. A.; Svergun, D. I. *Structure Analysis by Small-Angle X-ray and Neutron Scattering*; Plenum Press: New York, 1987.

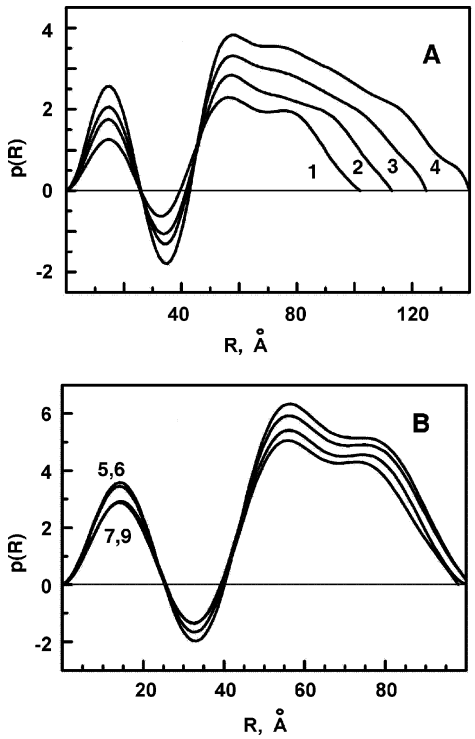

Figure 5. Distance distribution functions calculated from the SAXS curves shown at Figure 4 and corresponding to fits in Figure 4: (A) Nanodiscs formed with proteins **1**−**4**; (B) Nanodiscs formed with proteins **5**−**7** and **9**.

same geometry. Indeed, R_g for all Nanodiscs in Table 2 are almost equal to the Stokes radii, while for homogeneous globular particles they would be approximately 1.5 times smaller. This observation confirms the uneven distribution of electron density in Nanodiscs, which is expected for the protein surrounding lipid bilayer. The same conclusion follows from distance distribution curves shown in Figure 5. The shape of these curves is typical for lipid bilayers,[34,51] which have negative contrast at the central part of the particle and positive contrast at the edges. Maximal dimensions of scattering particles can be also estimated from Figure 5 as the maximum abscissa values where the function becomes equal to zero.

All curves at Figure 5 have similar shape at low *R*, indicating the similar density distributions for all disks. Particularly important are positions of the maxima at 55−57 Å, which are again the same for all Nanodiscs. The position of this maximum is determined by the lipid bilayer thickness, estimated from experimental data as 55 Å, using fits with various multilayered cylindrical models. The sizes of Nanodiscs obtained from these fits are also shown in Table 2. In agreement with the results on lipid/protein stoichiometry and SEC, the diameters of disks are very different for the set of extended proteins and do not change significantly for the truncation mutants described in this work. The bilayer thickness calculated from SAXS is 55−59 Å for all Nanodiscs with DPPC as the incorporating phospholipid. This value is in good agreement with the published thickness of the DPPC bilayer [39,55] and with the thickness of similar Nanodiscs determined by atomic force microscopy (AFM) on a mica surface earlier in our laboratory.[56,57] The bilayer heights, derived from SAXS curves for Nanodiscs formed with POPC (Table 2), are also consistent with the published data on POPC bilayers in a liquid crystalline state in ambient conditions. The control experiments with Nanodiscs formed with DMPC and MSP1 resulted in similar density distribution curves, with the expected shift of this maximum to smaller *R*, 51 Å, indicating the thickness of the DMPC bilayer as 50 Å (data not shown).

On the contrary, the oblate ellipsoidal core−shell models show different density distribution functions, with maximum at 60−75 Å, which changes for Nanodiscs of different sizes. The comparison of calculated model functions with experimental data fits shown in Figures 4 and 5 strongly favors the topology of Nanodiscs as a cylinder with flat bilayer surfaces, as opposed to the convex ellipsoidal particle. This is in line with many other indications of the presence of phospholipid bilayer in such lipid/protein discoidal particles, including the observation of characteristic gel−liquid crystal phase transitions[58,59] and the results of NMR,[47] polarized absorption, and fluorescence spectroscopy.[60,61]

As a result, SAXS with Nanodiscs of different sizes provides strong support for the structural model of the Nanodisc as a fragment of lipid bilayer surrounded by a helical protein belt. The length of the scaffold protein serves as a determinant for the diameter of the lipid/protein particle, while the thickness is precisely the same for all particles, despite a 2-fold difference in mass. These features are the direct consequence of the self-assembly process of this system, with a cylindrical fragment of the flat DPPC bilayer solubilized in aqueous solution by the protein helix interacting with the hydrophobic rim of the lipid cylinder.

All features of the experimental SAXS curves could be successfully fitted, using models such as that shown at Figure 1. Equally good fits were obtained also with the cylindrical shell model with six parameters, four electron densities, the diameter of the Nanodisc, and mean bilayer thickness (see Experimental Section). Models with fewer parameters, as well as spherical and ellipsoidal shell models, built without the fractional geometrical restrictions based on experimentally observed stoichiometry of the particles, were in disagreement with the known volume fractions of apolar acyl chains, phosphocholine polar heads, and the protein scaffold. From the known composition of lipid/protein particles one can calculate the total volumes of protein, phosphatidylcholine polar heads, and apolar acyl chains, each having specific electron density. The parameters obtained with the cylindrical model are in good agreement with the sizes estimated using other methods and electron densities reported for DPPC bilayers at the ambient conditions. Thus, the inability of ellipsoidal models to meet the constraints imposed by experimentally determined Nanodisc compositions provides additional evidence that they contain a cylindrical fragment of lipid bilayer surrounded by two continuous protein helices. Although SAXS can rarely provide unambiguous proof

(55) Sun, W. J.; Suter, R. M.; Knewtson, M. A.; Worthington, C. R.; Tristram-Nagle, S.; Zhang, R.; Nagle, J. F. *Phys. Rev. E* **1994**, *49*, 4665−4676.
(56) Bayburt, T. H.; Sligar, S. G. *Proc. Natl. Acad. Sci. U.S.A.* **2002**, *99*, 6725−6730.
(57) Bayburt, T. H.; Carlson, J. W.; Sligar, S. G. *Langmuir* **2000**, *16*, 5993−5997.
(58) Dergunov, A. D.; Taveirne, J.; Vanloo, B.; Hans, C.; Rosseneu, M. *Biochim. Biophys. Acta* **1997**, *1346*, 131−146.
(59) Andrews, A. L.; Atkinson, D.; Barratt, M. D.; Finer, E. G.; Hauser, H.; Henry, R.; Leslie, R. B.; Owens, N. L.; Phillips, M. C.; Robertson, R. N. *Eur. J. Biochem.* **1976**, *64*, 549−563.
(60) Bayburt, T. H.; Sligar, S. G. *Protein Sci.* **2003**, *12*, 2476−2481.
(61) Koppaka, V.; Silvestro, L.; Engler, J. A.; Brouillette, C. G.; Axelsen, P. H. *J. Biol. Chem.* **1999**, *274*, 14541−14544.

in favor of one specific structural model, as compared to all other possible structures,[38,62] in our case independent fits of the whole family of topologically similar particles strongly support the model shown at Figure 1.

The SAXS results obtained for the Nanodiscs formed with truncated scaffold proteins are shown in Figure 4B. Contrary to Figure 4A, all of the experimental curves appear almost identical, and the fits return very similar parameters. Notably, the disks formed with the shortest truncated protein MSP1D2 (**9**−**11**), in which 22 N-terminal amino acids were removed, have slightly smaller sizes as well as the number of lipids per disk, although the difference between these disks and all others formed with MSP1 (**1**, **5**, **6**) and MSP1D1 (**7**, **8**) is much smaller than it could be according to the differences between their contour lengths. The disk size independence on the presence or absence of the first 20 N-terminal amino acids was observed on several truncated proteins and proves that these residues are not necessary for the formation of lipid/protein Nanodiscs, at least at the optimal conditions, when the structurally homogeneous monodisperse disks are formed. The special properties of the corresponding region of the native human apo A-1 protein have been described in the thorough study of Nolte and Atkinson,[63] in which they reported that the predicted helix forming propensity of this part is not high enough to expect a stable amphipathic helical segment. However, in the X-ray crystal structure of the truncated lipid-free apo A-1,[44] all these residues except the first five were assigned to a helical conformation and later were commonly considered a "first helix", presumably interacting with the lipid in discoidal particles similarly to the rest of the protein.[18,21] Our results show that the presence of the first 22 N-terminal amino acids is not mandatory for the formation of monodisperse Nanodiscs at the optimum protein−lipid stoichiometry ratio. We cannot exclude that this first helix interacts with the lipids and takes part in stabilization of larger discoidal particles, which are formed at higher lipid/protein ratio in the assembly mixture. This mechanism could explain multiple sizes of lipid/protein disks, formed in apparently similar conditions, as noted previously.[16,18,20,21,64,65] This size heterogeneity, together with the presence of cholesterol in many such preparations and in vivo, would result in different structure and stability of these lipoprotein models, thus changing their susceptibility to the enzymes of lipid and cholesterol metabolism.[66]

Discussion

We undertook the systematic engineering of encircling amphipathic helical proteins that solubilize and support discoidal lipid bilayers in order to define the fundamental structural requirements of the membrane scaffold protein which control the resulting size, shape, and stability of the self-assembled lipid−protein nanostructures. Although the important conclusions reached in these investigations have significant impact on the study of natural human lipoprotein structures such as HDL particles, the overreaching goal of this work was to generate optimized sequences of scaffold proteins which can assemble disks of desired size for the ultimate incorporation of membrane protein targets. Our initial starting point used a scaffold protein[14] designed on the basis of truncated human Apo A-1 and synthetic lipid DPPC. Subsequent designs, however, used systematic variation of the scaffold protein sequence as well as a variety of phospholipids. Protein variants included insertion and deletion of amphipathic helical segments of different length. We also utilized lipids with various structures to vary the bilayer melting temperature and overall lipid packing density.

All data strongly support the proposed structural model of a "belt" wrapping of the membrane scaffold protein around the circumference of a phospholipids bilayer which renders the composite self-assembled nanostructure soluble in aqueous solution. In this model the length of the helical protein belt defines the size of the lipid fragment so encompassed. The average surface area per lipid, which is of course different for various lipids, then determines the number of lipids incorporated into the Nanodisc and consequently the optimal stoichiometry of protein/lipid packing. The genetic constructions reported herein, which systematically alter the length of the membrane scaffold protein, and the subsequent structural analysis by precise determination of component stoichiometry, size exclusion chromatography, and solution X-ray scattering defines uniquely a viable model for the resultant faithful self-assembly of lipids and amphipathic helical proteins into nanoscale particles. Such information is valuable, not only to those interested in the natural mechanisms of human lipoprotein assembly but also to those interested in the design of molecularly complex yet homogeneous systems for the study of membrane proteins and associated biological processes.

The size distribution of self-assembled lipid−protein particles as a function of the lipid/protein ratio in the initial mixture as studied by HPLC shows the critical importance of the initial stoichiometry of the lipid and protein components in the formation of monodisperse Nanodiscs with high yield. At the optimum lipid/protein ratio, where the yield of discoidal particles is highest, the result of the self-assembly process is a homogeneous and monodisperse ensemble which contains exactly the number of lipids necessary to form the well-packed interior of a discoidal lipid bilayer surrounded by two protein molecules. Notably, in these Nanodisc structures, we determine that not all parts of the original scaffold protein molecules interact with the hydrophobic rim of lipid bilayer. In particular, the truncated proteins **7**−**11**, as well as the proteins without the hexa-His tag and linker, are able to envelop exactly the same number of lipid molecules as the parent structures based on the MSP1.[14] Almost exactly the same Nanodisc structures are formed by scaffold proteins that vary in lengths from 178 to 223 amino acids (see Table 2, and compare Nanodiscs formed by **1** and **5**−**11**).

As expected the N-terminal tag and associated linker sequences are not critical for the formation of Nanodiscs of defined size. An important new result, however, is the fact that the first helical region composed of the initial first approximately 20 amino acids in the sequence of original MSP1 (**1**) do not take part in formation of the helical scaffold protein belt. In contrast, additional amphipathic helical protein sequences which are inserted into the core membrane scaffold protein sequence result in larger solubilized bilayer structures. For example, when additional 22-mers are inserted in the middle of the MSP1

(62) Volkov, V. V.; Svergun, D. I. *J. Appl. Crystallogr.* **2003**, *36*, 860−864.
(63) Nolte, R. T.; Atkinson, D. *Biophys. J.* **1992**, *63*, 1221−1239.
(64) Jonas, A.; Wald, J. H.; Toohill, K. L.; Krul, E. S.; Kezdy, K. E. *J. Biol. Chem.* **1990**, *265*, 22123−22129.
(65) Jonas, A.; von Eckardstein, A.; Kezdy, K. E.; Steinmetz, A.; Assmann, G. *J. Lipid Res.* **1991**, *32*, 97−106.
(66) Jonas, A. *Biochim. Biophys. Acta* **2000**, *1529*, 245−256.

sequence (Table 2, proteins **2**−**4**), each additional helix results in a dramatic increase of the optimum lipid/protein ratio and the number of lipid molecules in Nanodiscs. The corresponding structural changes, as determined by solution X-ray scattering, provide additional support for the model of an encircling "belt" of solubilizing amphipathic helices.

An important feature of all lipid titration experiments reported herein is the dominant position of the main fraction, corresponding to the optimal lipid/protein ratio reported in Table 2, at which the Nanodiscs are formed with the highest yield. Experiments with all of the scaffold proteins summarized in Table 2 show the presence of this main size fraction, even at much higher than optimal lipid/protein ratios. These even include those assembly stoichiometries which would be calculated for discoidal structures formed from three, four, or more molecules of the membrane scaffold proteins assembling per disk. Hence, there is a clear advantage in the formation of Nanodiscs with only two scaffold proteins per discoidal unit over other lipid/protein stoichiometries which require a larger number of MSP equivalents.

The exact molecular details of the self-assembly process are, as yet, imperfectly understood. The overall process is complex and reflects thermodynamic preferences for different conformations of scaffold proteins in lipid-free and lipid-bound states, as well as kinetic factors, which may turn out to be the determinant of self-assembly under most conditions. For example, the gradual decrease of cholate concentration presumably results in the formation of lipid bilayer fragments with correspondingly increasing size. Thus the scaffold protein, which competes with cholate as the stabilizer of the lipid bilayer rim, can interact with smaller bilayer fragments and form smaller Nanodiscs with only two proteins per disk earlier, than with bigger fragments, which may form only later in the course of dialysis. If the protein concentration is high enough, the scaffold protein can successfully replace cholate and form smaller disks. If there is not enough scaffold protein, then the bigger disks with three and four protein molecules per disk can also be formed, as was observed experimentally at high lipid/protein ratios in assembly mixture. The kinetics of these processes is clearly important, as the overall yield of homogeneous Nanodiscs depends on the rate of cholate removal (unpublished observations).

The thermodynamic driving force of the bilayer disk self-assembly is the minimization of the protein−lipid interface and of the corresponding energy penalty.[67,68] The optimum lipid/protein ratio in the assembly mixture is determined by the geometry of the resultant Nanodiscs, namely, the contour length of the protein amphipathic helix, i.e., the protein component of the disk, and the average surface area per lipid molecule in bilayer at the given conditions. Understanding which parts of the composite helical scaffold proteins contribute to the defining features of the resultant discoidal assemblies opens new possibilities for directed self-assembly of similar lipid/protein Nanodiscs with controlled size. Our results obtained with the series of extended proteins as described in this paper provide a proof-of-principle for such supramolecular design and suggest that the output of such self-assembly processes may be finely tuned with respect to the critical determinants of the corresponding phase diagram. In addition, more than two components with different properties may be used in the similar way, including the incorporation of integral membrane proteins,[60] peripheral membrane proteins,[56] and other compounds which can partition into a lipid bilayer.

Discoidal lipid micelles have also been studied in binary systems where the second component, either detergent, a phospholipid with shorter chain length, or various polymers, etc., served as stabilizers for the rim of the disk. In the membrane scaffold protein system described herein, however, the protein helical length is the sole determinant of disk size while at the same time maintaining the fidelity of the self-assembly process which results in a narrow, monodisperse size distribution. Another important aspect is the stability of these self-assembled discoidal bilayer particles. There are indications of thermodynamic instability of discoidal phospholipid micelles,[50,69,70] which have been suggested to aggregate and transform into vesicles or lamellar phase, depending on numerous exogenous factors. With protein instead of surfactant stabilizing the rim of a phospholipids bilayer, as occurs in the MSP solubilized Nanodiscs, the overall stability is dramatically increased.

In conclusion, we have obtained information on the composition and structure of a series of monodisperse lipid/protein molecular complexes, termed Nanodiscs, which result from a systematic variation of an encircling amphipathic helical protein component. Systematic variation of the length of the MSP results in the predicted structural changes of the self-assembled bilayer Nanodisc. Precise measurements of the composition of these Nanodiscs revealed new details for the interaction of scaffold protein with lipid, including the fact that an initial 20 amino acids and the N-terminal of the human Apo-AI sequence are not involved in the generation of a stable protein−lipid interface and are not important for the self-assembly of Nanodiscs from detergent-solubilized mixtures. These observations are supported by solution X-ray scattering, which provides an independent characterization of size, shape, and structure. It is unambiguously shown that DPPC molecules in Nanodiscs form a phospholipids bilayer with the flat surface and the thickness identical to that measured for lamellar and vesicular samples in gel phase.[39,71] At the same time, slightly higher values obtained for the surface area per lipid molecule in Nanodiscs suggest the structural perturbation of the lipid packing at the protein−lipid interface, which could be expected from the mismatch between the height of hydrophobic acyl chains of DPPC in bilayer and the diameter of the protein helix.

One of the most important consequences of our work is the possibility to form monodisperse lipid/protein Nanodiscs of desired size and composition as a result of directed self-assembly of components solubilized in aqueous-detergent solutions. The size of the disks may be controlled through protein engineering, as well as various functionalization pathways can be added at the N-terminal fragment, which was shown to be neutral with respect to the lipid scaffolding. Similar results were obtained using a variety of phospholipid lipids with varying degrees of gel or liquid crystalline state.[14,60] The membrane scaffold protein

(67) May, S. *Eur. Biophys. J.* **2000**, *29*, 17−28.
(68) Kralchevsky, P. A.; Paunov, V. N.; Denkov, N. D.; Nagayama, K. *J. Chem. Soc., Faraday Trans.* **1995**, *91*, 3415−3432.
(69) Leng, J.; Egelhaaf, S. U.; Cates, M. E. *Europhys. Lett.* **2002**, *59*, 311−317.
(70) Leng, J.; Egelhaaf, S. U.; Cates, M. E. *Biophys. J.* **2003**, *85*, 1624−1646.
(71) Bouwstra, J. A.; Gooris, G. S.; Bras, W.; Talsma, H. *Chem. Phys. Lipids* **1993**, *64*, 83−98.

directed assembly of nanoscale solubilized phospholipids bilayers offers a versatile system for the study of lipid−protein interactions and a promising tool for solubilization and molecular studies of the critical components of biological membranes, such as enzymes, receptors, ion channels, and other molecules of interest for biology, medicine, and nanosciences.[56,60,72]

Acknowledgment. Portions of this work were performed at the DuPont-Northwestern-Dow Collaborative Access Team (DND-CAT) Synchrotron Research Center located at Sector 5 of the Advanced Photon Source. DND-CAT is supported by the E.I. DuPont de Nemours & Co., The Dow Chemical Co., the U.S. National Science Foundation through Grant DMR-9304725, and the State of Illinois through the Department of Commerce and the Board of Higher Education Grant IBHE HECA NWU 96. Use of the Advanced Photon Source was supported by the U.S. Department of Energy, Basic Energy Sciences, Office of Energy Research under Contract No. W-31-102-Eng-38. We gratefully acknowledge the help and support provided by Dr. J. Quintana, Dr. D. Keane, and Dr. S. Weigand while working at Argonne. Important discussions with Dr. T. Bayburt are gratefully acknowledged. We gratefully acknowledge the support of the Northwestern University Nanoscale Science and Engineering Center and Duke University and of Dr. L. Pesce, who developed the preliminary models for Nanodisc scattering experiments and analysis. The work was supported from NIH Grant GM33775 to S.G.S.

Supporting Information Available: Amino acid sequence of MSP1, experimental protocols for expression and purification of TEV protease and for N-terminal tag cleavage using TEV protease, HPLC separation curves for self-assembly mixtures with different scaffold proteins and different lipid/protein ratios (PDF). This information is available free of charge via the Internet at http://pubs.acs.org.

JA0393574

(72) Civjan, N. R.; Bayburt, T. H.; Schuler, M. A.; Sligar, S. G. *BioTechniques* **2003**, *35*, 556−563.